SCIENTIFIC REPORTS

OPEN

Dysregulated JAK2 expression by TrkC promotes metastasis potential, and EMT program of metastatic breast cancer

Received: 18 February 2016
Accepted: 02 September 2016
Published: 22 September 2016

Min Soo Kim[1], Joon Jeong[2], Jeongbeob Seo[3], Hae-Suk Kim[4], Seong-Jin Kim[5] & Wook Jin[1,6]

Metastatic breast cancers are aggressive tumors associated with high levels of epithelial-mesenchymal transition (EMT) markers, activation of IL6/JAK2/STAT3 and PI3K/AKT pathways for cell growth, mobility, invasion, metastasis, and CSC status. We identified a new molecular and functional network present in metastasis that regulates and coordinates with TrkC. Inhibition of SOCS3-mediated JAK2 degradation by TrkC increases total JAK2/STAT3 expression, and then leads to upregulation of Twist-1 through activation of JAK2/STAT3 cascade. Also, TrkC increases secretion and expression of IL-6, suggesting that this autocrine loop generated by TrkC maintains the mesenchymal state by continued activation of the JAK2/STAT3 cascade and upregulation of Twist expression. Moreover, TrkC interacts with the c-Src/Jak2 complex, which increases Twist-1 and Twist-2 levels via regulation of JAK2/STAT3 activation and JAK2/STAT3 expression. Furthermore, TrkC enhances metastatic potential of breast cancer via induction of EMT by upregulating Twist-1 and Twist-2. Additionally, TrkC significantly enhances the ability of breast cancer cells to form pulmonary metastases and primary tumor formation. Unexpectedly, we found that TrkC expression and clinical breast tumor pathological phenotypes show significant correlation. These findings suggest that TrkC plays a central role in tumorigenicity, metastasis, and self-renewal traits of metastatic breast cancer.

Metastatic breast cancers have shown enriched gene signatures that are responsible for cell-cell adhesion and markers linked to stem cell function and the EMT program[1,2]. By activating a usually dormant EMT program, carcinoma cells can acquire phenotypes that have therapeutic resistance, stem cell-like characteristics that are required for the execution of most steps of the invasion–metastasis cascade[2,3]. In addition, EMT-inducing transcription factors such as Snail[4–6], Slug[7,8], SIP1[9,10], Goosecoid[11,12], FOXC2[13], Twist-1[14], and Twist-2[15] can promote this transition.

The recent discovery of cancer stem cells (CSCs) in neoplastic tissues suggests a key role of stem cells in tumorigenesis and metastasis. Importantly, the induction of EMT by EMT-inducing transcription factors can spontaneously convert both normal and neoplastic non-stem cells into a stem-like state. In addition, acquisition of CSC subpopulations, which are present in some human breast tumors, is associated with disease aggressiveness and poor survival[2,16,17]. Moreover, CSCs are more enriched in metastatic breast cancer cells. Furthermore, the IL-6/JAK2/Stat3 pathway was preferentially active in metastatic breast cancer cells, and inhibition of JAK2 decreased the number of cells and blocked the growth of xenografts[18].

TrkC belongs to the tropomyosin-related kinase (Trk) family of neurotrophin receptors that primarily regulates growth, differentiation, and survival of neurons[19]. Trk family members have also been found in several

[1]Laboratory of Molecular Disease and Cell Regulation, Department of Biochemistry, School of Medicine, Gachon University, Incheon 406-840, Korea. [2]Department of Surgery, Gangnam Severance Hospital, Yonsei University Medical College, 712 Eonjuro, Gangnam-Gu, Seoul, 135-720, Korea. [3]Medicinal Chemistry, CMG Pharma, 335, CHA Bio Complex, Pangyo-ro, Bundang-gu, Seongnam-si, Gyeonggi-do, 13488, Korea. [4]TheragenEtex Bio Institute, TheragenEtex Co., Suwon, Gyeonggi-do 16229, Republic of Korea. [5]Nano-Bio Medicine Research Center, Advanced Institutes of Convergence Technology, and Department of Transdisciplinary Studies, Graduate School of Convergence Science and Technology, Seoul National University, Suwon, Kyunggi-do 16229, Republic of Korea. [6]Gachon Medical Research Institute, Gil Medical Center, Incheon, 405-760, Korea. Correspondence and requests for materials should be addressed to S.-J.K. (email: jasonsjkim@snu.ac.kr) or W.J. (email: jinwo@gachon.ac.kr)

non-neural cell types, such as brain cancer, soft tissue cancer, and lung cancer[20–23]. In addition, recent studies have identified several somatic mutations in TrkC implicated in breast (R678Q)[24,25], lung (V307L, H677Y, L336Q, R721F)[25,26], gastric (T149R)[25], colorectal (G608S, I695V, R731Q, K732T, L760I)[27], and pancreatic (G608S, E322K, H599Y)[28–30] cancers. These results suggest that TrkC may have high mutation rates in human cancer genomes and can be potentially activated by somatic mutations. Furthermore, TrkC may function as a dominant cancer gene that is activated by genetic rearrangements in cancer. Although TrkC mutations have been identified in a number of human tumors, it is unclear whether deregulated TrkC is oncogenic. We recently demonstrated that TrkC expression activates mitogenic and survival pathways in breast cancer cells. We have also shown that TrkC rendered cells resistant to TGF-β tumor suppressor activity, suggesting that suppression of the TGF-β tumor suppressor pathway may contribute to TrkC-mediated tumorigenicity[31]. Furthermore, we recently demonstrated that c-Src activation by TrkC induces activation of the PI3K-AKT pathway[32]. These findings indicate that TrkC activation/overexpression may play a crucial role in the initiation, progression, and metastasis of breast cancer and other tumors. However, the signaling mechanisms that induce and maintain tumorigenicity and metastasis of breast cancer by TrkC have remained poorly understood. In this study, we show that TrkC was highly expressed in metastatic breast cancer and that TrkC may contribute to the conversion of breast cancer cells into a more aggressive and chemoresistant form via acquirement of mesenchymal characteristics and metastatic ability. Thus, our study uncovers and functionally dissects a new molecular and functional network present in cancer metastasis mediated by TrkC.

Results

TrkC expression was correlated with pathological phenotypes of breast cancer. Although our previous studies have already demonstrated that TrkC plays a crucial role in initiation, progression, and metastasis of cancer by inducing activation of the PI3K-AKT cascade[32] and Twist-1 expression[33], TrkC expression patterns have not been well characterized in human breast cancer. To assess whether TrkC was an important mediator of the metastatic potential of breast cancer, we first examined TrkC expression in a panel of established metastatic and non-metastatic human tumor cell lines. TrkC was highly expressed in basal-like breast cancer cell lines (MDA-MB-435, MDA-MB-231, Hs578T, SUM149, SUM159, and BT549) than in luminal cancer cell lines (BT474 and T47D). Immortalized human mammary epithelial cells (HMLEs) also expressed low to undetectable TrkC levels (Figure S1a). Next, we examined whether some of breast cancer cell lines used in our studies carry *TrkC* mutations. We conducted the bioinformatical analysis of our unpublished whole transcriptome data generated from human breast cancer cell lines. The sequencing analysis showed only synonymous variants in ZR-75HS578T cells (Table S1).

Based on the above observations, we speculated whether TrkC correlated with breast cancer pathology in breast cancer patients. Interestingly, TrkC expression was elevated in 14 out of 17 tumors (82%) relative to their corresponding patient-matched normal tissue samples (Fig. 1a). We next performed an *in silico* analysis of TrkC transcript levels in the tissues of 2,136 breast cancer patients of the Curtis dataset[34] and 473 breast cancer patients of the UNC dataset[1] at Oncomine. Strikingly, TrkC expression was more highly upregulated in basal and claudin-low breast cancers than in other breast cancer subtypes (Fig. 1b). These results suggested that TrkC expression was closely correlated with the TrkC gene signature derived from breast cancer subtypes.

Metastatic breast cancers are aggressive, chemoresistant tumors characterized by lineage plasticity and a unique molecular profile. Intersestingly, they also form a distinct subtype closely related to a novel subset of receptor-negative breast cancers (claudin-low) characterized by loss of genes involved in cell-cell adhesion[1]. Based on these observations, we evaluated whether TrkC expression correlated with a triple-negative subtype of breast cancer. TrkC expression was significantly elevated in triple-negative tumor tissues compared to normal tissue samples (Fig. 1c). Also, results from a large clinical microarray study showed that TrkC expression was significantly upregulated in triple-negative subtypes relative to other subtypes (Fig. 1d). Moreover, we evaluated TrkC expression in a series of 59 breast cancer samples by immunohistochemistry. We found a significant correlation between TrkC expression and pathological phenotypes. Normal breast tissue samples demonstrated weak immunoreactivity to an anti-TrkC antibody; however, high TrkC levels were detected in infiltrating ductal and metastatic carcinoma samples (Fig. 1e). Furthermore, results from a large clinical microarray study showed that patients with tumors exhibiting high TrkC expression levels exhibit poorer survival outcomes relative to patients with tumors expressing low TrkC levels (Fig. 1f). Our observation indicated that patients with higher TrkC expression have worse prognosis relative to those that have low TrkC expression and it might play a crucial role in progression and metastasis of breast cancer.

TrkC induces Twist by inducing activation and expression of JAK2/STAT3. To investigate the relationship between JAK2/STAT3 cascade and TrkC-induced Twist-1 expression, we first assessed the effects of a Trk inhibitor and JAK2 inhibitor on JAK2/STAT3 activation and JAK2/STAT3/Twist-1 expression. The inhibition of TrkC activation by K252a in Hs578T and SUM149 cells significantly reduced JAK2/STAT3 phosphorylation and Twist-1 expression. Interestingly, JAK2 and STAT3 expression levels were markedly reduced upon treatment with K252a (Fig. 2a). Also, the inhibition of JAK2 activation in Hs578T and SUM149 cells by the JAK2 inhibitor AG490 significantly reduced JAK2 and STAT3 phosphorylation and Twist-1 expression (Fig. 2b). However, JAK2 and STAT3 expression levels were not significantly different after treatment with AG490. Moreover, the inhibition of TrkC activation by K252a in MCF10A-TrkC cells significantly reduced JAK2/STAT3 phosphorylation and Twist-1 expression. Also, JAK2 and STAT3 expression levels were markedly reduced upon treatment with K252a (Fig. 2c). These results suggest that the tyrosine kinase activity of TrkC correlates with increased expression levels of JAK2 and STAT3.

To examine whether TrkC knockdown could influence the activation of JAK2/STAT3/Twist cascade, we selected highly metastatic Hs578T and SUM149 cells stably expressing TrkC-shRNAs. As shown in Figure S1b,

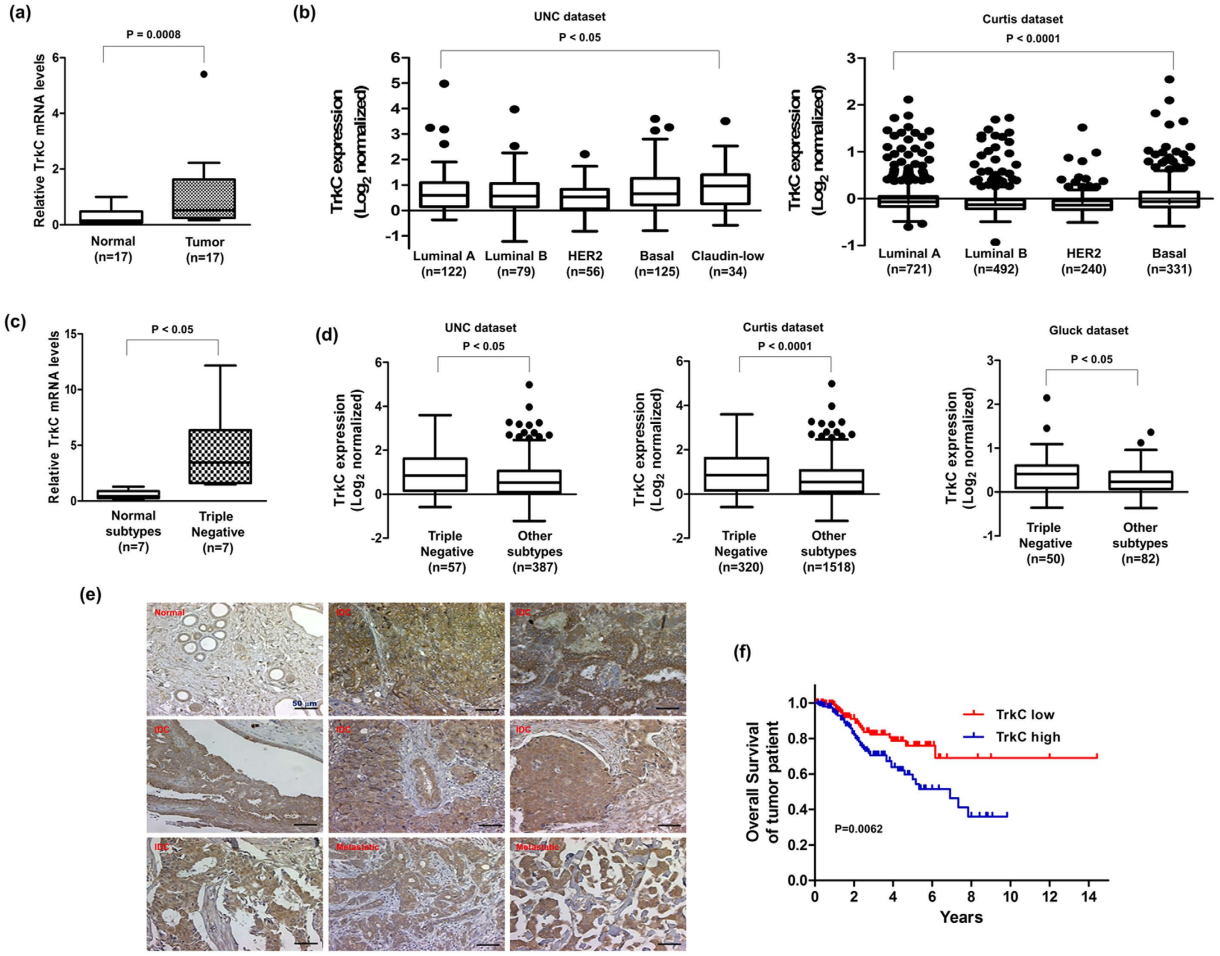

Figure 1. Increased expression of TrkC in human breast carcinomas. (**a**) Relative levels of TrkC expression in normal or invasive breast carcinoma samples of 17 individual breast cancer patients. The expression was compared to that of healthy tissue, and the endogenous 18S mRNA level was measured as an internal control. A *P* value was considered to be significant in *t*-test. (**b**) The gene expression data were plotted as Box-and-whisker (Tukey) plots of mean TrkC expression levels in molecular subtypes of breast cancer patients. The signatures of TrkC level extracted from 2,136 Curtis and 473 UNC datasets and averaged for each tumor. Points below and above the whiskers are drawn as individual dots. A *P* value was considered to be significant in ANOVA. (**c**) Relative TrkC mRNA expression in seven individual normal human tissues or triple-negative breast carcinoma samples. The endogenous 18S mRNA level was measured as an internal control. A *P* value was considered to be significant in *t*-test. (**d**) The mean TrkC expression in other subtypes or triple-negative subtypes of human breast cancer patients from three publicly available data sets (Curtis, Gluck, and UNC datasets). The TrkC gene expression level was extracted from the dataset and averaged for each tumor. Points below and above the whiskers are drawn as individual dots. A *P* value was considered to be significant in *t*-test. (**e**) Pattern of TrkC expression in a series of 59 breast cancer samples. Representative immunohistochemical images of TrkC staining in normal human breast tissue, infiltrating duct carcinoma, and metastatic carcinoma in the lymph nodes (magnification: 200×). (**f**) Patients were divided into those who expressed high and low TrkB levels, and their survival rates from a publicly available data set (UNC) were compared. The *P* value was calculated by a log-rank test.

TrkC-shRNA suppressed the expression of endogenous TrkC by 70%. Immunoblotting analysis revealed that JAK2 and STAT3 phosphorylation levels were markedly reduced in Hs578T and SUM149 TrkC-shRNA cells relative to those in control-shRNA cells. Interestingly, JAK2, STAT3, and Twist expression levels were also significantly reduced in Hs578T and SUM149 TrkC-shRNA cells (Fig. 2d).

To determine whether tyrosine kinase activity of TrkC was important for the induction of JAK2 and STAT3 expression, we ectopically expressed TrkC, TrkC K572N, or TrkC Yx3F mutants in MCF10A. In the activation-loop tyrosine triple mutant, TrkC Yx3F, all three activation-loop tyrosines were mutated to phenylalanine. In mutant TrkC K572N, an ATP-binding site residue, lysine 572 (K), was substituted with asparagine (N). Interestingly, JAK2/STAT3 expression and activation were markedly reduced in MCF10A-TrkC K572N and MCF10A-TrkC Yx3F compared to that in MCF10A-TrkC cells (Fig. 2e). Also, activation and expression of JAK2/STAT3 and Twist-1 expression were significantly increased in Hs578T and SUM149 TrkC-shRNA cells by ectopically-expressed TrkC, but not the TrkC K572N or TrkC Y3XF mutants (Fig. 2f). These findings suggest that

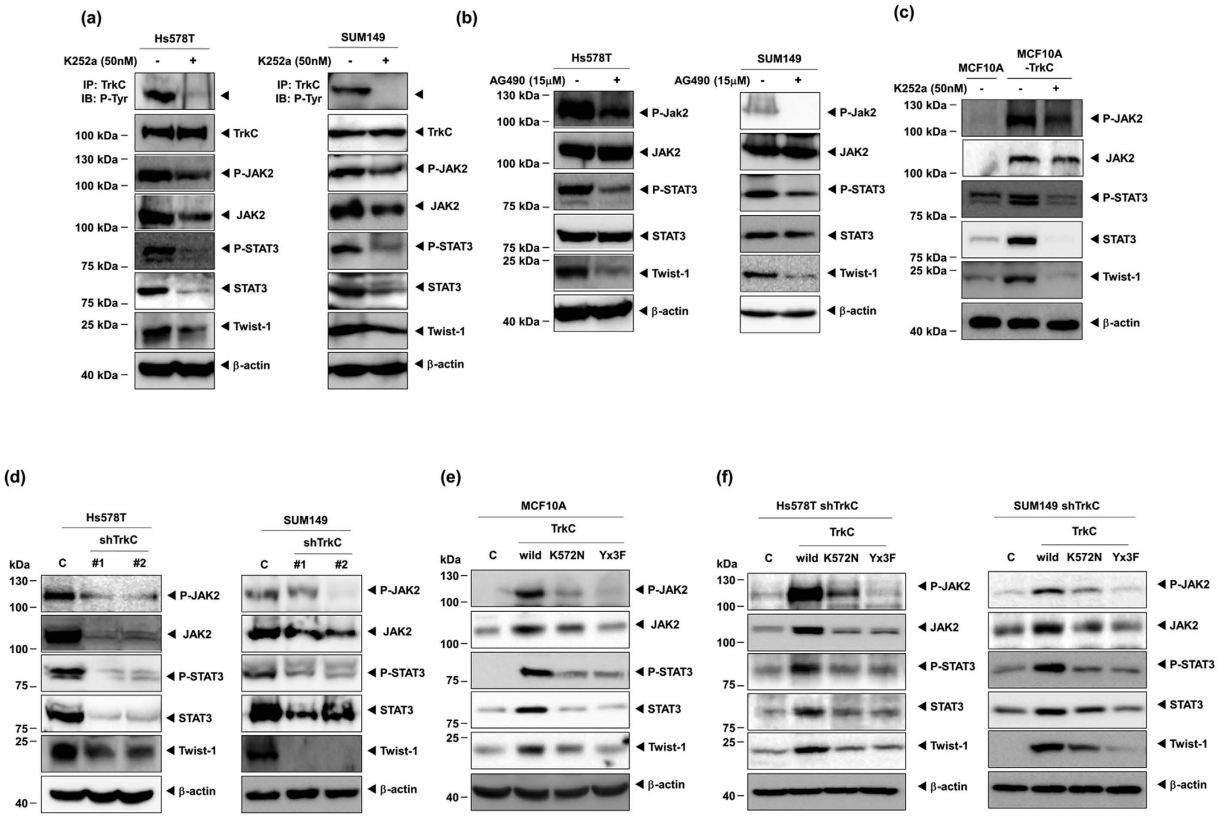

Figure 2. TrkC regulates JAK2/STAT3 activity and directly regulates its downstream target. (**a**) Western blot analysis of the expression of P-JAK2, JAK2, P-STAT3, STAT3, and Twist-1 proteins in Hs578T and SUM149 cells with or without 50 nM K252a treatment for 16 hr. β-actin was used as a loading control. (**b**) Western blot analysis of the expression of P-JAK2, JAK2, P-STAT3, STAT3, and Twist-1 proteins in Hs578T and SUM149 cells with or without 15μM AG490 (JAK2 inhibitor) treatment for 16 hr. β-actin was used as a loading control. (**c**) Western blot analysis of the expression of P-JAK2, JAK2, P-STAT3, STAT3, and Twist-1 proteins in MCF10A or MCF10A-TrkC cells with or without 50 nM K252a treatment for 16 hr. β-actin was used as a loading control. (**d**) Western blot analysis of the expression of P-JAK2, JAK2, P-STAT3, STAT3, and Twist-1 proteins in Hs578T and SUM149 control-shRNA or TrkC-shRNA cells. β-actin was used as a loading control. (**e**) Western blot analysis of the expression of P-JAK2, JAK2, P-STAT3, STAT3, and Twist-1 proteins in MCF10A, MCF10A-TrkC, or MCF10A-TrkC kinase-dead mutant (K572N, Yx3F) cells. β-actin was used as a loading control. (**f**) Western blot analysis of the expression of the proteins P-JAK2, JAK2, P-STAT3, STAT3, and Twist-1 in SUM149 and Hs578T control-shRNA or TrkC-shRNA cells after transfection of TrkC or TrkC kinase-dead mutant (K572N, Yx3F) constructs.

the tyrosine kinase activity of TrkC is required for JAK2/STAT3/Twist-1 induction. Furthermore, STAT3 mRNA expression was markedly reduced in response to TrkC knockdown (Figure S2a). Additionally, STAT3 luciferase activity was significantly decreased in SUM149 and Hs578T TrkC-shRNA cells relative to SUM149 and Hs578T control-shRNA cells (Figure S2b). These observations suggest that TrkC induces not only STAT3 phosphorylation but also STAT3 transcription. Because inhibition of JAK2 activity downregulates STAT3 phosphorylation but not STAT3 transcription, the transcriptional induction of STAT3 by TrkC is independent of the JAK2 signaling pathway.

TrkC induces JAK2 stabilization via inhibition of SOCS3-mediated ubiquitination. Because TrkC knockdown reduced JAK2 protein levels, we next examined whether TrkC transcriptionally regulated JAK2 expression in SUM149 and Hs578T TrkC-shRNA cells. TrkC knockdown had no effect on JAK2 mRNA levels in SUM149 and Hs578T TrkC-shRNA cells (Fig. 3a). Interestingly, activation and expression of JAK2 and STAT3 in Hs578T and SUM149 control-shRNA or TrkC-shRNA cells increased upon treatment with the proteasome inhibitor MG132 (Figure S3b), suggesting that TrkC post-translationally controls JAK2 protein stability. JAK2 ubiquitination leads to degradation of the JAK2 protein; therefore, we investigated whether JAK2 stabilization by TrkC was mediated through the suppression of JAK2 ubiquitination. TrkC kinase-dead mutants (K572N, Y3XF) or K252a treatment significantly induced JAK2 ubiquitination compared to TrkC wild type (Fig. 3c and S3b). Furthermore, SOCS3 mediates the negative feedback inhibition of the JAK-STAT pathway. Specifically, induced SOCS3 protein can bind to JAK2 and suppress its activity by directly binding to its catalytic center and promoting its proteasomal degradation[35]. As shown in Fig. 3c, TrkC suppressed JAK2 ubiquitination, even in the presence of SOCS3.

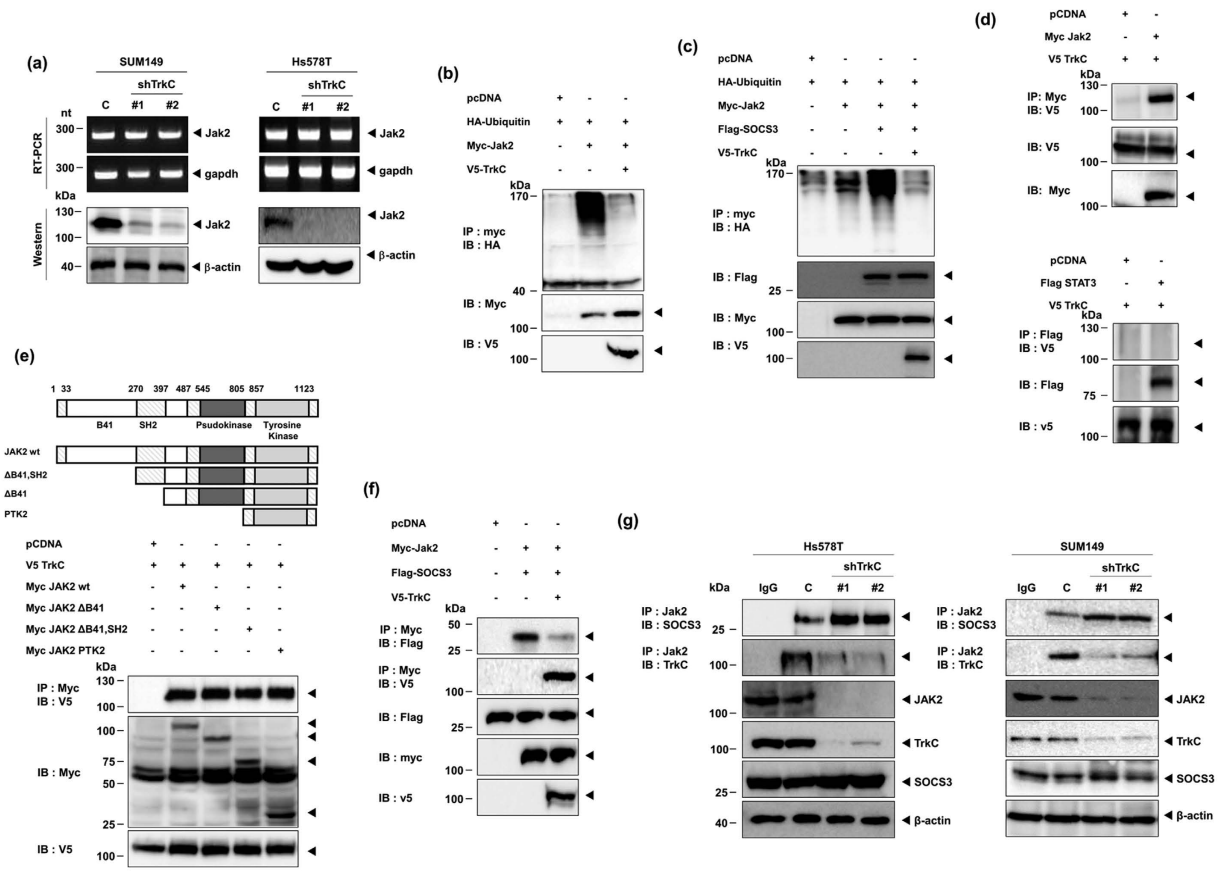

Figure 3. TrkC induces JAK2 stabilization by inhibiting SOCS3-mediated degradation of JAK2. (**a**) RT-PCR and western blot analysis of JAK2 expression in Hs578T and SUM149 control-shRNA or TrkC-shRNA cells. GAPDH and β-actin were used as loading controls. (**b**) Immunoblot analysis of whole-cell lysates and immunoprecipitates derived from 293T cells transfected with V5-TrkC, HA-Ubiquitin, and Myc-Jak2 constructs as indicated. (**c**) Immunoblot analysis of whole-cell lysates and immunoprecipitates derived from 293T cells transfected with V5-TrkC, HA-Ubiquitin, Flag-SOCS3, and Myc-Jak2 constructs as indicated. (**d**) TrkC interacts with JAK2. Immunoblot analysis of whole-cell lysates and immunoprecipitates derived from 293T cells transfected with the V5-TrkC and Myc-Jak2 constructs as indicated. (**e**) Identification of the JAK2 region responsible for TrkC interaction and immunoblot analysis of whole-cell lysates and immunoprecipitates derived from 293T cells transfected with the V5-TrkC and Myc-Jak2 deletion constructs as indicated. (**f**) Identification of the inhibition of SOCS3-JAK2 complex formation by TrkC and immunoblot analysis of whole-cell lysates and immunoprecipitates derived from 293T cells transfected with the V5-TrkC, Flag-SOCS3, and Myc-Jak2 constructs as indicated. (**g**) Identification of endogenous SOCS3-JAK2 complexes in Hs578T and SUM149 control-shRNA or TrkC-shRNA cells.

We aimed to determine whether TrkC induced JAK2 activation by blocking the ability of SOCS3 to ubiquitinate and degrade JAK2 through the SOCS3-JAK2 complex formation. To test this possibility, we first examined whether TrkC directly interacts with JAK2. As shown in Fig. 3d, TrkC directly interacts with JAK2 but not with STAT3. However, TrkC kinase dead mutants and K252a treatment significantly reduced JAK2 interaction relative to TrkC wild type (Figure S3c).

To identify the JAK2 functional domain responsible for its interaction with TrkC, we used a series of JAK2 deletion constructs. TrkC interacted with the tyrosine kinase domain of JAK2, but did not interact with the B41, SH2, or pseudokinase domain of JAK2 (Fig. 3e). We next investigated whether TrkC inhibited the formation of the SOCS3-JAK2 complex. As expected, TrkC coexpression significantly reduced the level of SOCS3 that associated with JAK2 (Fig. 3f). We next compared JAK2-SOCS3 complex formation in SUM149 and Hs578T TrkC-shRNA cells to that of control-shRNA cells. Relative to control-shRNA cells, endogenous levels of SOCS3 that associated with JAK2 were dramatically increased in SUM149 and Hs578T TrkC-shRNA cells (Fig. 3g). These results indicate that TrkC binds to JAK2 and inhibits proteasome-mediated JAK2 degradation by blocking SOCS3-JAK2 complex formation, leading to increased JAK2 protein levels and activation of the JAK2/STAT3/Twist-1 pathway.

TrkC increases IL-6 secretion and regulates the nuclear translocation of STAT3. The autocrine signal loop of IL-6 secreted by cancer cells induces STAT3 activation. Consequently, phosphorylated STAT3 translocates to the nucleus and participates in DNA binding, which culminates in transactivation of genes involved in

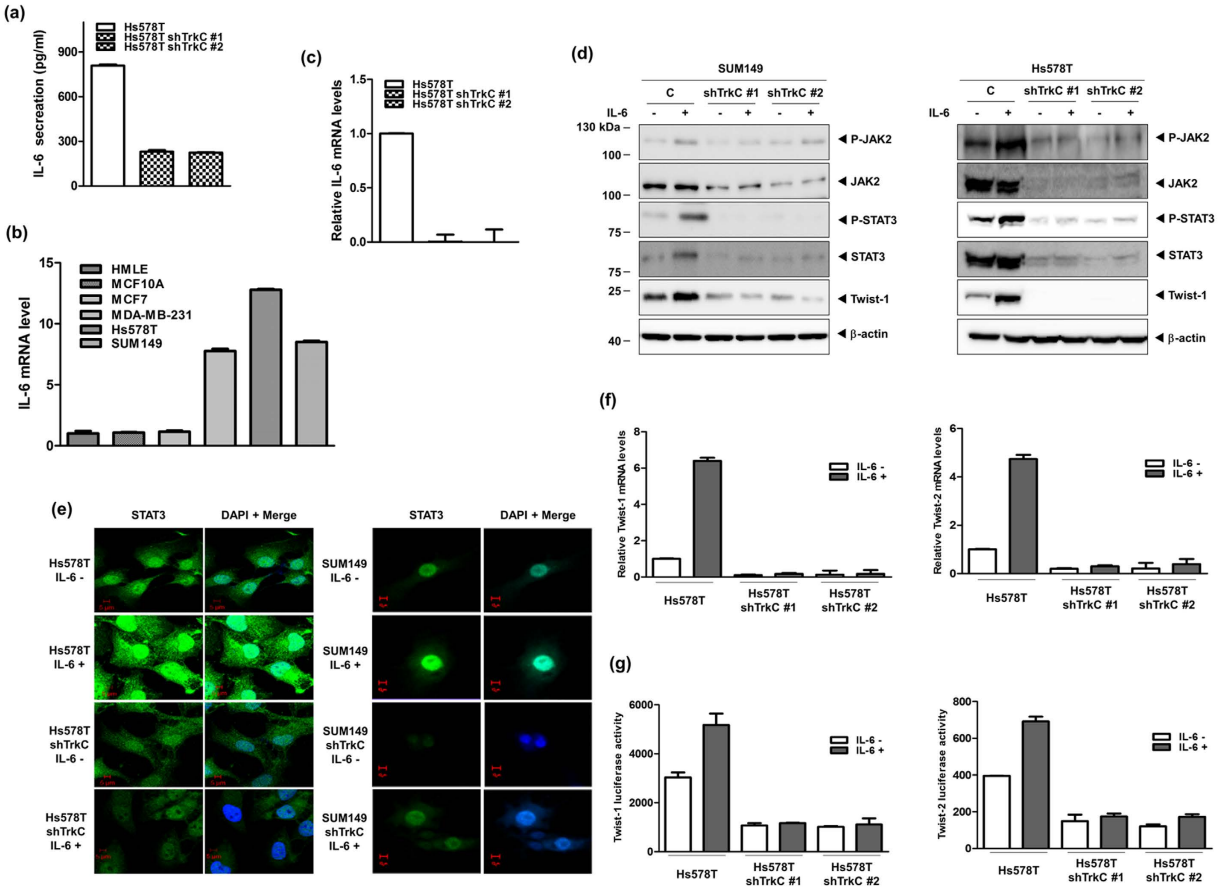

Figure 4. Increased secretion of IL-6 by TrkC correlates with increased nuclear translocation of STAT3. (**a**) ELISA assay of IL-6 secretion by Hs578T control-shRNA or TrkC-shRNA cells (n = 3). Data are presented as mean ± standard error of the mean (SEM). (**b**) Expression levels of mRNA encoding IL-6 in basal-like breast cancer cells (MDA-MB-231, MDA-MB-435, Hs578T, and SUM149) and normal or nontransformed cells (HMLE, MCF7, or MCF10A breast cells). 18S mRNA was used to normalize variability in template loading. Data are presented as mean ± standard error of the mean (SEM). (**c**) Expression levels of mRNA encoding IL-6 in Hs578T control-shRNA or TrkC-shRNA cells. 18S mRNA was used to normalize variability in template loading. Data are presented as mean ± standard error of the mean (SEM). (**d**) Western blot analysis of the expression of P-JAK2, JAK2, P-STAT3, STAT3, and Twist-1 proteins in Hs578T and SUM149 control-shRNA or TrkC-shRNA cells with or without IL-6 treatment. β-actin was used as a loading control. (**e**) Immunofluorescence staining of the nuclear translocation of STAT3 in Hs578T and SUM149 control-shRNA or TrkC-shRNA cells with or without IL-6 treatment. The green signal represents staining of the corresponding protein, while the blue signal represents DAPI nuclear DNA staining. (**f**) Expression levels of mRNA encoding Twist-1 and Twist-2 in Hs578T control-shRNA or TrkC-shRNA cells with or without IL-6 treatment. 18S mRNA was used to normalize variability in template loading. Data are presented as mean ± standard error of the mean (SEM). (**g**) Luciferase reporter assay of Twist-1 and Twist-2 in Hs578T control-shRNA or TrkC-shRNA cells with or without IL-6 treatment. Each bar represents the mean ± SEM of three experiments. Data are presented as mean ± standard error of the mean (SEM). Some of the bar graphs do not have visible error bars due to low values of standard error of the mean (SEM).

a number of cellular functions, such as proliferation, differentiation, survival, and maintenance of CSCs[18,36–40]. Therefore, we speculated that maintenance of JAK2/STAT3 activation might depend on the activation of the IL-6 autocrine signaling loop by TrkC. To test this notion, we tested IL-6 levels secreted into the culture medium of Hs578T control-shRNA or TrkC-shRNA cells. Hs578T control-shRNA cells exhibited increased secretion of IL-6 protein relative to Hs578T TrkC-shRNA cells (Fig. 4a).

We next tested whether TrkC expression in highly metastatic breast cancer cells may affect the expression of IL-6. To investigate this possibility, we compared IL-6 mRNA expression in highly metastatic breast cancer cells to that of normal or nontransformed cells. Relative to those in normal or nontransformed cells (HMLE, MCF7, or MCF10A), the levels of IL-6 were dramatically increased in highly metastatic breast cancer cells (MDA-MB-231, Hs578T, and SUM149), which highly express TrkC (Figure S1a and 4b). However, IL-6 mRNA expression in Hs578T control-shRNA cells was markedly increased relative to that in Hs578T TrkC-shRNA cells (Fig. 4c).

To further examine TrkC-mediated regulation of the JAK2/STAT3 pathway, we assessed JAK2 and STAT3 activation following treatment of SUM149 and Hs578T control-shRNA cells or TrkC-shRNA cells with IL-6. IL-6 treatment dramatically increased JAK2 and STAT3 phosphorylation levels in SUM149 and Hs578T

control-shRNA cells relative to those in SUM149 and Hs578T TrkC-shRNA cells (Fig. 4d). Moreover, we examined whether enhanced IL-6 by TrkC actually activates the JAK2/STAT3 pathway. The levels of phospho-JAK2 and STAT3 were more decreased in SUM149 and Hs578T control-shRNA or TrkC-shRNA cells after treatment with IL-6 neutralizing monoclonal antibody (Figure S4). These results suggest that enhanced IL-6 secretion by TrkC required maintenance of tumorigenicity and metastasis through activation of the JAK2/STAT3 and PI3K/AKT pathways and Twist-1 expression. Furthermore, STAT3 nuclear translocation after IL-6 treatment was markedly increased in SUM149 and Hs578T control-shRNA cells relative to SUM149 and Hs578T TrkC-shRNA cells (Fig. 4e). Additionally, the expression of JAK2, STAT3, Twist-1, and Twist-2 was markedly increased in Hs578T control-shRNA cells, but not in Hs578T TrkC-shRNA cells (Fig. 4d,f), which was correlated with the increased luciferase activity of Twist-1 and Twist-2 in Hs578T control-shRNA cells (Fig. 4g).

TrkC activates the JAK2/STAT3/Twist-1 axis directly and indirectly through c-Src. STAT3 activation by activated c-Src led to a significant increase in the levels of phospho-STAT3 and Twist-1[41]. Also, in our previous study, endogenous TrkC interacted with c-Src, and the suppression of TrkC expression resulted in a marked repression of c-Src activation[32]. Therefore, we speculated that TrkC/c-Src and STAT3 might be functionally linked to the regulation of Twist-1 and Twist-2 expression. To test this, we evaluated whether c-Src in the presence of TrkC played a functional role in the induction of Twist by STAT3 activation. As shown in Fig. 5a, STAT3 phosphorylation levels were markedly decreased after treatment of SUM149 and Hs578T cells with SU6656, an inhibitor of c-Src. Twist-1 expression was markedly decreased as well; however, STAT3 expression was not affected by SU6656 treatment. Interestingly, we found that JAK2 phosphorylation and expression levels were markedly decreased after treating SUM149 and Hs578T cells with SU6656. To further examine whether c-Src regulated the activation and expression of JAK2 and STAT3, we first selected highly metastatic Hs578T and SUM149 cells stably expressing c-Src-shRNAs. As shown in Figure S5a, Hs578T and SUM149 c-Src-shRNA significantly suppressed the expression of endogenous c-Src. Also, immunoblotting analysis revealed that JAK2 and STAT3 phosphorylation levels were markedly reduced in Hs578T and SUM149 c-Src-shRNA cells relative to those in control-shRNA cells. Moreover, expression levels of JAK2 and Twist, but not STAT3, were significantly reduced in Hs578T and SUM149 c-Src-shRNA cells (Figure S5b), which was correlated with SU6656 treatment. Our results suggested that both TrkC and c-Src are required for the induction of JAK2/STAT3 expression and activation. Therefore, we next examined the possibility that TrkC/c-Src interacts with JAK2. As shown in Fig. 5b, TrkC/c-Src interacted with JAK2 after transient transfection. In addition, JAK2 interacted with TrkC in the absence of c-Src, indicating the direct binding of TrkC to JAK2. Also, endogenous TrkC interacted with endogenous c-Src/JAK2 in SUM149 and Hs578T cells (Fig. 5c).

To confirm the role of c-Src in TrkC-mediated JAK2 activation, we overexpressed TrkC or c-Src in SYF cells derived from triple knockout mouse embryos lacking c-Src, Yes, and Fyn (Klinghoffer *et al.* 1999). To further determine whether TrkC-JAK2 formed a complex in the absence of c-Src, we transiently transfected SYF-TrkC and SYF-c-Src-TrkC cells with JAK2. As shown in Fig. 5d, TrkC-JAK2 complexes were detected in both c-Src-deficient SYF-TrkC and SYF-c-Src-TrkC cells. Next, we investigated whether TrkC induced activation of JAK2 without c-Src. The activation and expression of JAK2 were markedly increased in SYF-TrkC cells, and TrkC directly activated JAK2 via TrkC/JAK2 complex formation without c-Src (Fig. 5e). To further confirm the role of TrkC in the activation of the JAK2/STAT3 pathway, we examined the activation of JAK2/STAT3/Twist-1 in SYF-TrkC cells and SYF-c-Src-TrkC cells. TrkC-mediated JAK2 and STAT3 phosphorylation levels and expression were markedly increased in SYF-TrkC cells. These levels were further enhanced in SYF-c-Src-TrkC cells, suggesting that TrkC/c-Src or TrkC synergistically induced JAK2/STAT3 phosphorylation. Consistent with these results, Twist-1 and Twist-2 expression was markedly increased when TrkC and c-Src were co-expressed (Fig. 5f,g). Moreover, Hs578T TrkC-shRNA cells demonstrated lower Twist-1 and Twist-2 mRNA levels than Hs578T cells treated with SU6656 (Fig. 5h). Furthermore, Twist-1 and Twist-2 luciferase activity in Hs578T control-shRNA and TrkC-shRNA cells were slightly reduced after SU6656 treatment (Figure S6a). However, Twist-1 and Twist-2 luciferase activity was markedly increased in SYF-TrkC cells and SYF-c-Src-TrkC cells (Figure S6b). Taken together, our results suggest that TrkC can activate the JAK2/STAT3/Twist-1 axis directly and indirectly through c-Src.

TrkC enhances metastatic potential of breast cancer through induction of EMT program. During cancer pathogenesis, a transdifferentiation program known as EMT is activated, thus enabling cells to execute multiple steps of the invasion-metastasis cascade. EMT refers to a complex molecular and cellular program in which epithelial cells shed their differentiated characteristics, including cell–cell adhesion, planar and apical–basal polarity, and lack of motility. The epithelial cells instead acquire mesenchymal features, which include motility, invasiveness, and a heightened resistance to apoptosis[42]. Our aforementioned observations suggested that TrkC may be sufficient to induce EMT. To address whether TrkC is sufficient to induce EMT, we ectopically expressed TrkC in MCF10A breast cancer cells and Maden-Darby Canine Kidney (MDCK) epithelial cells, which have been widely used to study EMT in breast cancer[12–14]. As shown in Fig. 6a, MCF10A and MDCK control cells expressed high levels of E-cadherin, α-catenin, and β-catenin, but minimal levels of N-cadherin and fibronectin. However, MCF10A-TrkC and MDCK-TrkC cells downregulated the expression of E-cadherin, α-catenin, and β-catenin, but increased N-cadherin and fibronectin expression. Moreover, MDCK-TrkC cells downregulated the expression of mRNA levels encoding epithelial marker (E-cadherin) while upregulating mRNA levels encoding mesenchymal marker (N-cadherin) (Fig. 6b).

The loss of E-cadherin appears to be critical for EMT. One major mechanism for inhibiting E-cadherin expression involves silencing of E-cadherin transcription through three E-boxes in CDH-1 promoter[43]. To determine whether the loss of E-cadherin in the MDCK-TrkC cells was due to transcriptional repression by upregulated

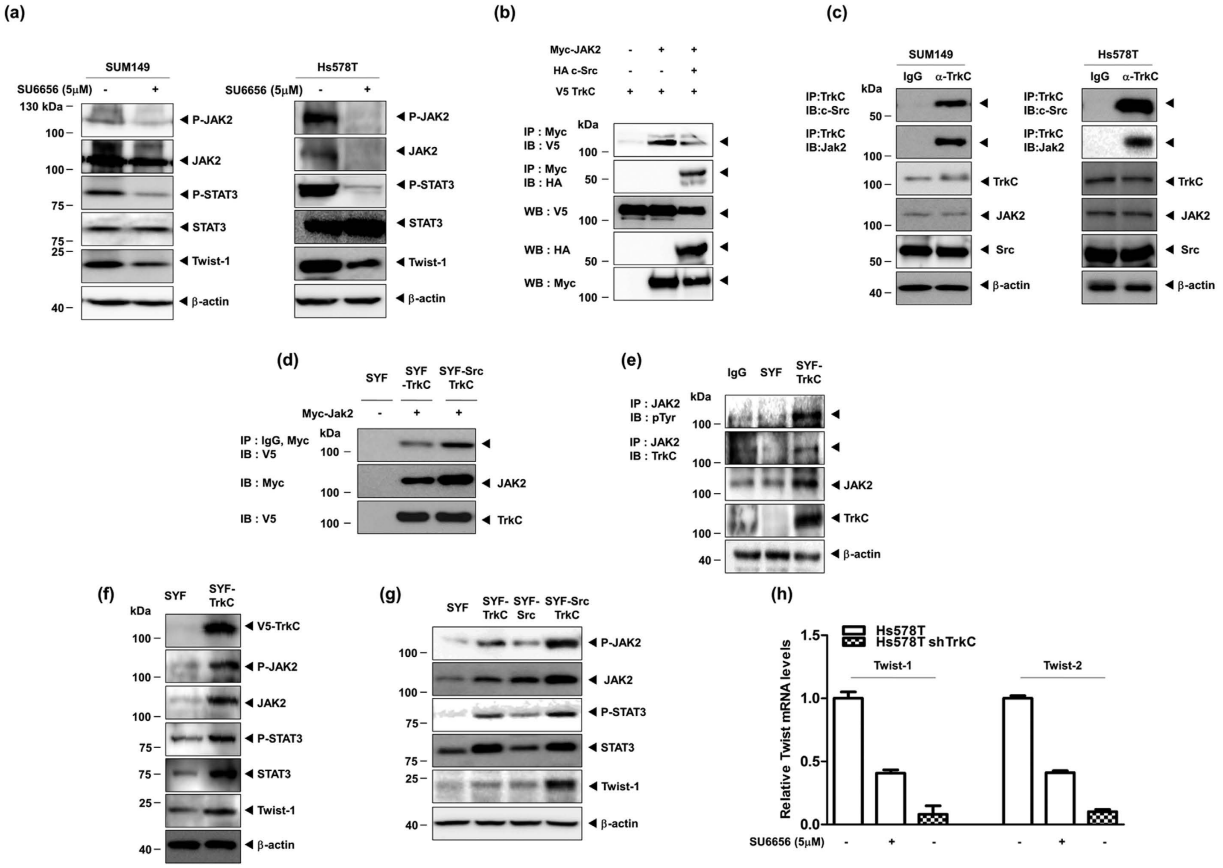

Figure 5. TrkC/c-Src or TrkC interacts with JAK2 and leads to Twist-1 upregulation through activation of the JAK/STAT3 pathway. (**a**) Western blot analysis of the expression of P-JAK2, JAK2, P-STAT3, STAT3, and Twist-1 proteins in Hs578T and SUM149 cells with or without 5 μM SU6656 treatment for 6 hr. β-actin was used as a loading control. (**b**) TrkC or TrkC/c-Src complex interacts with JAK2. Immunoblot analysis of whole-cell lysates and immunoprecipitates derived from 293T cells transfected with the V5-TrkC, HA c-Src, and Myc-Jak2 constructs as indicated. (**c**) Identification of complex formation of endogenous TrkC/c-Src/JAK2 in Hs578T and SUM149 cells. (**d**) TrkC interacts with JAK2 in SYF-TrkC cells or SYF-Src-TrkC cells after transfection with Myc-Jak2. (**e**) Activation and expression of Jak2 in SYF cells or SYF-TrkC cells after immunoprecipitation was examined by immunoblotting using the indicated antibodies. (**f**) Western blot analysis of the expression of P-JAK2, JAK2, P-STAT3, STAT3, and Twist-1 proteins in SYF cells or SYF-TrkC cells. (**g**) Western blot analysis of expression of P-JAK2, JAK2, P-STAT3, STAT3, and Twist-1 proteins in SYF, SYF-TrkC, SYF-cSrc, and SYF-cSrc-TrkC cells. (**h**) Expression levels of mRNA encoding Twist-1 and Twist-2 in Hs578T control-shRNA or TrkC-shRNA cells with or without 5 μM SU6656 treatment for 6 hr. 18S mRNA was used to normalize variability in template loading. Data are presented as mean ± standard error of the mean (SEM).

TrkC, we transiently transfected MDCK-TrkC cells with an E-cadherin reporter construct. Indeed, luciferase activity was efficiently suppressed in MDCK-TrkC cells compared to that in MDCK control cells (Fig. 6c). At the biochemical level, E-cadherin protein disappeared from the cell membrane in MDCK-TrkC cells but was strongly stained in the control cells. In contrast, N-cadherin expression was strongly induced in MDCK-TrkC cells (Fig. 6d). Therefore, the molecular changes in TrkC-expressing MDCK cells indicated that these cells had undergone EMT.

The major mechanism underlying the loss of E-cadherin mRNA is direct transcriptional repression by the repressors SIP1, Slug, Goosecoid, E12, Snail, HMGA2, and Twist-1. These transcriptional repressors have been found to induce EMT *in vitro,* and their overexpression in a variety of human tumors is associated with increased tumor invasion, metastasis, and poor prognosis[42,44]. To test this, we examined the expression levels of SIP1, Goosecoid, Slug, and E12 in MDCK cells, but we found that the levels did not differ significantly between the MDCK control and MDCK-TrkC cells (Fig. 6e). However, expression and luciferase activity of Twist-1 and Twist-2 was significantly higher in MDCK-TrkC cells than MDCK control cells (Fig. 6f,g). These data indicate that TrkC is capable of inducing EMT through JAK2/STAT3/Twist cascade. Based on our previous observations, we speculated that TrkC might contribute to EMT and breast cancer progression. To test this notion, we next examined whether TrkC knockdown affected the ability of SUM149 and Hs578T cells to express Twist-1 and Twist-2. Quantitative RT-PCR analysis showed that the mRNAs encoding Twist-1 and Twist-2, which are master regulators of tumor metastasis and EMT, were markedly reduced in SUM149 and Hs578T TrkC-shRNA cells

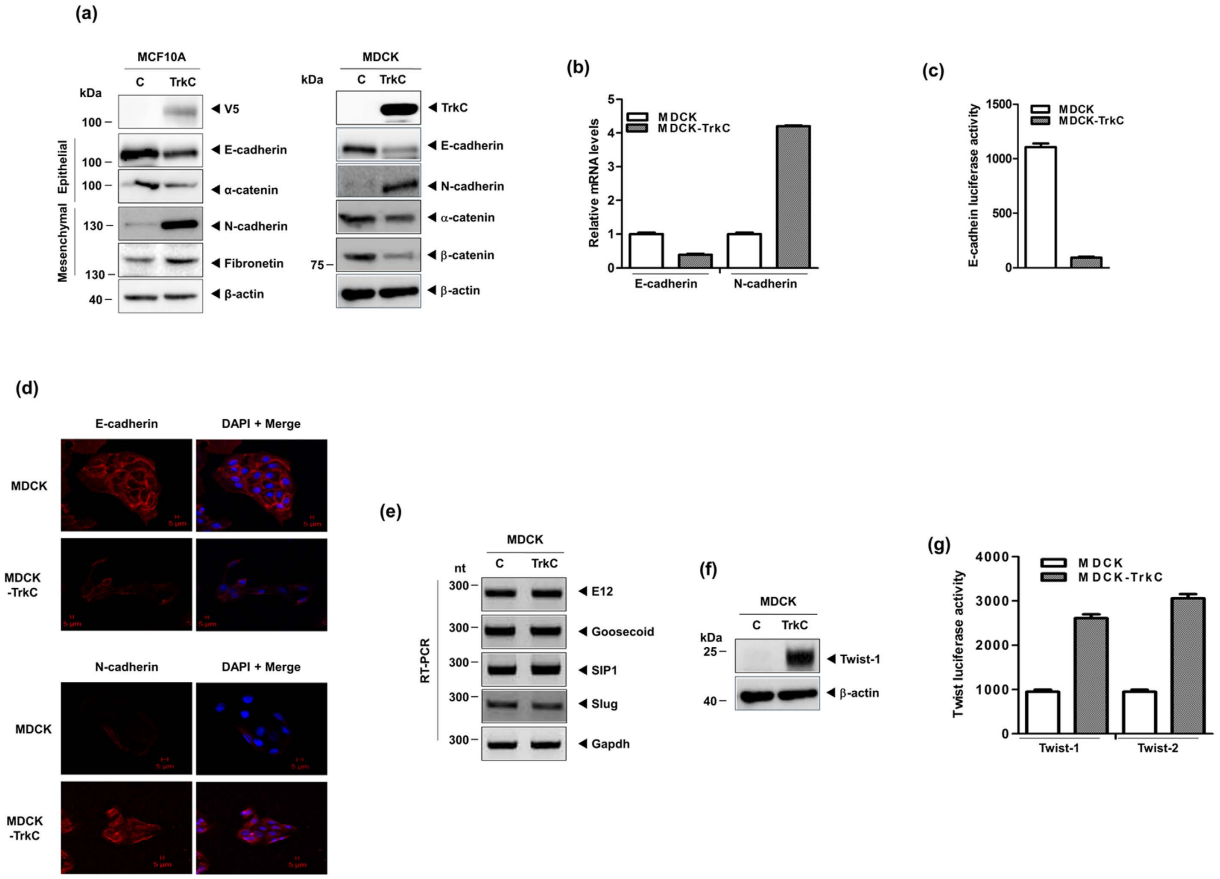

Figure 6. TrkC induces the EMT program by upregulating Twist. (**a**) Western blot analysis of the expression of TrkC, E-cadherin, α-catenin, β-catenin, N-cadherin, and fibronectin proteins in MCF10A and MDCK control or TrkC cells. β-actin was used as a loading control. (**b**) The expression levels of mRNA encoding E-cadherin and N-cadherin in MDCK or MDCK-TrkC cells. 18S mRNA was used to normalize variability in template loading. Data are presented as mean ± standard error of the mean (SEM). (**c**) Luciferase reporter assay of E-cadherin in MDCK or MDCK-TrkC cells. Each bar represents the mean ± SEM of three experiments. Data are presented as mean ± standard error of the mean (SEM). (**d**) Immunofluorescence staining of E-cadherin and N-cadherin in MDCK or MDCK-TrkC cells. The red signal represents the staining of the corresponding protein, while the blue signal represents DAPI nuclear DNA staining. (**e,f**) RT-PCR analysis of E12, Goosecoid, SIP1, or Slug mRNA levels (**f**) and immunoblotting analysis of Twist-1 levels (**f**) in MDCK or MDCK-TrkC cells. β-actin and GAPDH were used as loading controls. (**g**) Luciferase reporter assay of Twist-1 and Twist-2 in MDCK or MDCK-TrkC cells. Each bar represents the mean ± SEM of three experiments. Data are presented as mean ± standard error of the mean (SEM). Some of the bar graphs do not have visible error bars due to low values of standard error of the mean (SEM).

relative to those in control-shRNA cells (Figure S7a). As shown in Figure S7b, we also observed that Twist-1- and Twist-2 luciferase activity was efficiently and identically suppressed in SUM149 and Hs578T TrkC-shRNA cells compared to that of SUM149 and Hs578T control-shRNA cells. Moreover, immunofluorescence staining demonstrated that Twist-1 expression was high in Hs578T control-shRNA cells but was markedly reduced in Hs578T TrkC-shRNA cells (Figure S7c). A recent study demonstrated that the Twist-1 transcription factor, which is a master regulator of embryonic morphogenesis, plays an essential role in metastasis[14]. Induction of EMT by Immortalized human mammary epithelial cells (HMLEs) stably expressing Twist and Snail acquire self-renewing traits associated with normal tissue (SCs) and cancer stem cells (CSCs)[45]. Moreover, similar to Twist-1, Twist-2 is overexpressed in a large variety of human primary tumors and cancer cell lines[46]. These data indicate that TrkC is capable of inducing EMT through upregulation of Twist-1 and Twist-2 expression.

We next examined whether the pharmacological inhibition of TrkC with K252a, an inhibitor of Trk tyrosine kinases, could influence the ability of Hs578T cells to survive and proliferate. Hs578T cells proliferated as large spheroid aggregates in suspension but demonstrated a significantly lower survival outcome in suspension after treatment with the Trk inhibitor K252a. Also, Hs578T and SUM149 TrkC-shRNA cells showed markedly lower survival than Hs578T and SUM149 control-shRNA cells in suspension (Figure S8a). These findings suggest that TrkC affects Hs578T and SUM149 cell survival. We next examined whether the loss of TrkC expression affected the ability of Hs578T or SUM149 cells to proliferate *in vitro*. Hs578T and SUM149 TrkC-shRNA cells grew slower than Hs578T and SUM149 control-shRNA cells (Figure S8b). We also examined whether TrkC

knockdown affected the anchorage-independent growth of breast cancer cells. After growing in soft agar for 15 days, Hs578T control and SUM149 TrkC-shRNA cells formed a significantly lower number of colonies relative to that of the control (Figure S8c). To test for another functional hallmark of cancer, we conducted an *in vitro* motility assay and wound healing assays. Hs578T- and SUM149 control-shRNA cells showed increased cell motility, whereas Hs578T- and SUM149 TrkC-shRNA cells had low motility, indicating that the increased motility of cells was largely due to TrkC expression (Figure S8d,e). We next examined whether TrkC overexpression induces the metastatic potential of a non-metasizing breast cells. The capacity of the cell to migrate and invade was markedly reduced in MCF10A-TrkC kinase dead mutant cells (K572N, Yx3F), or MCF10A-TrkC cells treated with K252a had low motility (Figure S9a,b). Moreover, we examined whether TrkC overexpression enhances mammosphere-forming ability to acquirement of self-renewal trait associated with cancer stem cells (CSCs). MCF10A-TrkC cells significantly induced mammosphere-forming ability compared to the MCF10A and MCF10A kinase-dead mutant (K572N, Y3XF) cells or K252a treatment (Figure S9c).

TrkC is essential for primary tumor formation and metastasis of breast cancer. To determine the contribution of TrkC to primary tumor formation, we injected MCF10A-Ras, MCF10A-Ras-TrkC, Hs578T control-shRNA or TrkC-shRNA cells into the mouse mammary fat pads of BALB/c Nu/Nu mice and examined the resulting primary tumors 29 days or 47 days later. MCF10A-Ras-TrkC and Hs578T control-shRNA cells formed primary mammary tumors at identical rates, whereas the primary tumor formation of Hs578T TrkC-shRNA or MCF10A-Ras cells was markedly decreased (Fig. 7a–d). We next examined whether the pharmacological inhibition of TrkC with LOXO-101 could influence the ability of Hs578T cells to tumor growth *in vivo*. LOXO-101, a highly selective inhibitor of Trk tyrosine kinase, showed dramatic clinical activity in patients with a variety of cancers in phase I trials and is underongoing multicenter phase II trials[47]. Tumor growth *in vivo* by LOXO-101 treatment was dramatically inhibited relative to that of diluent (control) (Fig. 7e,f). These results demonstrate that TrkC is required for primary tumor formation of breast cancer.

To determine whether the loss of TrkC expression affected the ability of Hs578T cells to metastasize, Hs578T control-shRNA or TrkC-shRNA cells were injected into the tail veins of BALB/c Nu/Nu mice, and their lungs were examined for metastases 35 days later. The average number of visible metastatic nodules was markedly reduced in mice injected with Hs578T TrkC-shRNA cells relative to that of mice harboring Hs578T control-shRNA cells (Fig. 7g,h). Moreover, histological analyses confirmed that the number of micrometastatic lesions was drastically reduced in the lungs of mice with Hs578T TrkC-shRNA cells (Fig. 7h).

We suspected that the presence of small numbers of nodules in the lungs of mice carrying Hs578T TrkC-shRNA cells was due to incomplete knockdown of TrkC. Therefore, we analyzed TrkC expression in the lungs of mice expressing Hs578T control-shRNA or TrkC-shRNA cells. Although the few metastatic nodules that eventually formed in the lungs of mice with Hs578T TrkC-shRNA retained TrkC expression, TrkC expression in the lungs of mice with Hs578T TrkC-shRNA cells was drastically lower than that of Hs578T control-shRNA cells (Fig. 7i and S10a). These results indicate that TrkC loss reduces both cell motility and the number of metastases in the lung.

The regulation of Twist expression by TrkC was also evaluated by immunohistochemistry of the lungs of mice containing Hs578T control-shRNA or TrkC-shRNA cells using a Twist-1 specific antibody. Interestingly, Twist-1 expression was markedly reduced in the lungs of mice injected with Hs578T TrkC-shRNA cells compared to that of their control counterparts (Fig. 7i). Moreover, tumor cells expressed lower levels of Twist-1 and Twist-2 when isolated from the lungs of mice injected with Hs578T TrkC-shRNA cells rather than Hs578T control-shRNA cells (Figure S10b,c).

Discussion

In our previous work, TrkC was found to induce Twist-1 expression in breast cancer. However, the signaling mechanisms by which TrkC induces Twist-1 and Twist-2 have been unclear. Here, we found that TrkC was sufficient for direct interaction with JAK2 and blocked SOCS3-induced JAK2 degradation, which resulted in stabilization of JAK2 expression and induction of STAT3, as well as the upregulation of Twist-1 gene expression. SOCS3 is a transcriptional target of STAT3 that promotes the proteasomal degradation of phosphorylated STAT3 in a negative feedback loop[48–50]. Moreover, tissue remodeling was dramatically accelerated in *Socs3*-deficient mammary glands by activation and high levels of STAT3[51]. Furthermore, activated STAT3 transcriptionally induces Twist, which plays an important role in promoting metastasis and CSC traits[41,45,52]. Overall, we identified a new molecular and functional network present in cancer metastasis that regulates and coordinates with TrkC.

Recent studies have demonstrated that both autocrine and paracrine signals of IL-6 secreted by basal-like breast cancers lead to poor clinical outcome of basal-like breast cancers, and maintenance of stem cell–like cancer cells. Moreover, the positive feedback loop of IL-6 by NF-κB signaling is mediated by the activation of the JAK2/STAT3 and PI3K/AKT pathways, and triggers malignant features in mammosphere formation[18,36–40]. We hypothesized that the JAK2/STAT3 and PI3K/AKT pathways are activated in metastatic breast cancer cells due to IL-6 induction by TrkC and IL-6 subsequently activates an autocrine loop. We demonstrated that TrkC increases secretion and expression of IL-6, suggesting that these autocrine loops generated by TrkC may ensure maintenance of the mesenchymal/CSC state by continued activation of the JAK2/STAT3 and PI3K/AKT pathways and upregulation of Twist expression.

In our previous work, c-Src activation by TrkC was found to induce activation of the PI3K-AKT pathway[32]. Moreover, activated c-Src has been shown to induce STAT3 activation and lead to a significant increase in the levels of Twist-1 and Twist-2[41]. In addition, increased associations between c-Src and HER-2 contribute to trastuzumab resistance[53]. Therefore, we investigated whether induction of Twist-1 depended on the activation of STAT3 via c-Src activation by TrkC. Our findings indicated that activated c-Src by TrkC induced Twist expression

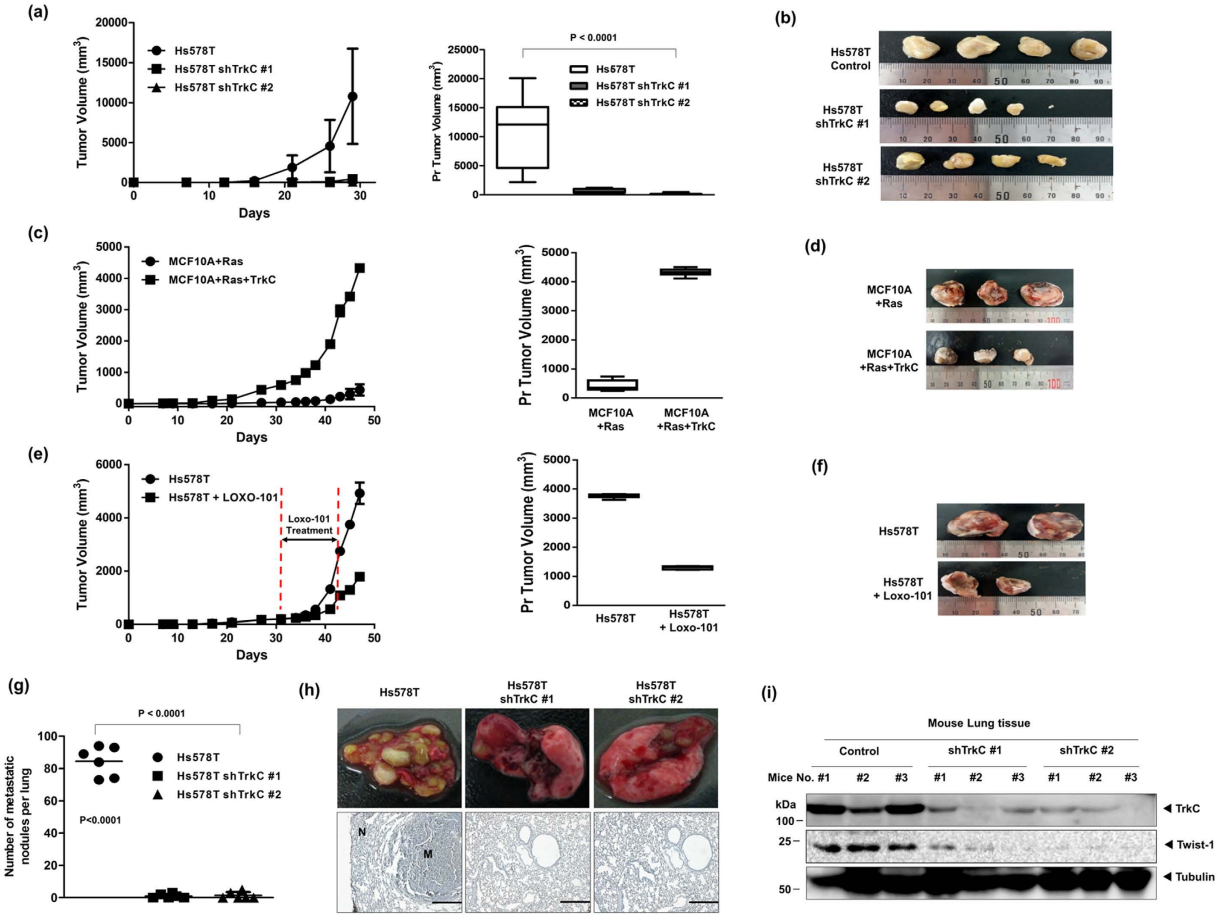

Figure 7. Suppression of TrkC expression inhibited the ability of Hs578T cells to metastasize from the mammary gland to the lung. (**a**) Volumes of primary mammary tumors formed by Hs578T control-shRNA or TrkC-shRNA cells. Each data point represents the mean of each type of primary tumor. A $P < 0.0001$ was considered to indicate significance for ANOVA. (**b**) Representative images of tumors from mice harboring Hs578T control-shRNA or TrkC-shRNA mammary tumors after tumor implantation. (**c**) Volumes of primary mammary tumors formed by MCF10A-Ras or MCF10A-Ras-TrkC cells. Each data point represents the mean of each type of primary tumor. A $P < 0.0001$ was considered to indicate significance for ANOVA. (**d**) Representative images of tumors from mice harboring MCF10A-Ras or MCF10A-Ras-TrkC cells. (**e**) LOXO-101 inhibits tumor growth in a Hs578T xenograft model. 1×10^6 cells were implanted into the mammary fat pads of mice and treated with diluent (control) or LOXO-101 (60 mg/kg/dose) twice daily for 14 days when the tumor size was $200 \pm 20\,mm^3$. (**f**) Representative images of tumors from mice harboring diluent (control) or LOXO-101 (60 mg/kg/dose) (**g**) Total number of lung metastatic nodules in each mouse in each group were counted using a dissection scope. Two populations of Hs578T cells that were independently infected with TrkC-shRNA #1 and TrkC-shRNA #2 were used in independent experiments (n = 6) and consistently yielded similar results. A $P < 0.0001$ was considered to indicate significance for ANOVA. (**h**) Representative images and H&E staining sections of mouse lung lobes 35 days after tail vein injection of Hs578T control-shRNA or TrkC-shRNA cells. N, Normal lung tissue; M, metastatic nodule. (**i**) Immunoblotting of the expression of TrkC and Twist-1 in tumor cells recovered from the lungs of individual mice expressing either Hs578T control-shRNA or TrkC-shRNA. Some of the bar graphs do not have visible error bars due to low values of standard error of the mean (SEM).

through induction of JAK2 expression, but not STAT3 activation. Our study further demonstrated that TrkC was a key regulator in the induction of Twist-1 through activation of JAK2 and STAT3. Moreover, we demonstrated that TrkC is associated with JAK2/c-Src and induces JAK2/c-Src activation, resulting in increased phospho-JAK2/STAT3 levels, which subsequently leads to Twist-1 upregulation. These observations suggest that TrkC can activate the JAK2/STAT3/Twist-1 axis directly and indirectly through c-Src.

Individual tumor cell invasion is a highly complicated process that requires malignant cells to, at minimum, obtain migration and dissemination properties to escape from the constraints of tissue structure[54]. We delineated the role of TrkC in cancer malignancies. TrkC knockdown markedly suppressed survival in suspension and primary tumor formation while significantly reducing micrometastatic lesions in mice injected with Hs578T TrkC-shRNA cells. Our data suggest that TrkC is sufficient for tumorigenicity and metastasis of breast cancer cells. Moreover, these findings shed new light on the role of TrkC in metastasis and the possibility that molecular

components of TrkC signaling pathways are potential candidates for future investigations, due to their possible involvement in tumor metastasis.

Taken together, we dissected the role of TrkC in EMT by gain-of-function ectopic TrkC overexpression. A number of studies suggest that carcinoma cells often activate EMT to acquire the ability to execute multiple steps of the invasion-metastasis cascade. EMT-mediated invasion has also been largely attributed to the loss of E-cadherin, a tumor invasion suppressor. In addition, EMT has been associated with cancer stem cell traits, suggesting a role of EMT in the initiation of recurrent tumors from disseminated cancer cells[3,42,45,55]. In this study, we demonstrated that TrkC plays a critical role in EMT. Indeed, during the induction of EMT, we observed activation of EMT-inducing transcription factors, notably Twist-1 and Twist-2. Increased Twist-1 and Twist-2 expression is found in various human cancers, including melanoma, T-cell lymphoma, rhabdomyosarcoma, and gastric carcinomas[56–58]. Additionally, Twist-1 and Twist-2 proteins override oncogene-induced premature senescence by abrogating key regulators of the p53- and Rb-dependent pathways. Moreover, in epithelial cells, the oncogenic cooperation between Twist proteins and activated mitogenic oncoproteins such as Ras and ErbB2 lead to complete EMT[14,15,46]. Furthermore, induction of EMT by Twist-1 induces and maintains stem cell states in breast cancer[45,52]. Our findings suggest that TrkC-induced EMT can contribute to the invasion and metastasis phenotypes.

Metastatic breast cancers enhances chemoresistance through upregulation of EMT markers and exhibit a $CD44^{high}/CD24^{low}$ antigenic phenotype with stem cell-like characteristics (CSCs). Activation of the PI3K/AKT pathway, IL-6/JAK2/STAT3 pathway, and stem cell-like characteristics contribute to the poor outcomes of metastatic breast cancers[1,18]. Therefore, it is likely that TrkC regulates the activity of JAK2/STAT3/Twist-1 and PI3K/AKT to generate relatively unlimited numbers of cancer stem cells, and to induce the metastatic potential of cancer cells through the induction of EMT (Figure S10). In addition, the inhibition of TrkC kinase activity may have a notable impact on the tumorigenic and metastatic capacities of highly metastatic breast cancers. Accordingly, the role of TrkC in the development and progression of human breast cancer deserves further attention.

Materials and Methods

All methods carried out in this manuscript were approved by Institutional Biosafety Committee and Institutional Animal Care and Use Committee (IACUC) of the Gachon University. In addition to this, all experiments were performed in accordance with the approved regulations and guidelines.

Cell culture and reagents. Human breast cancer cells (Table S2), SYF, 293T, and MDCK cells were purchased from American Type Culture Collection (Manassas, VA, UDA); SUM149 breast cells were obtained from Dr. Stephen Ethier (Kramanos Institute, MI, USA) and were maintained as described previously[14,59]. K252a, MG-132, SU6656, and AG490 were purchased from Calbiochem.

Human breast tumor samples. RNA of normal and tumorous human breast samples were obtained from the Gangnam Severance Hospital after approval by the institutional review board and the ethics committee of Gangnam Severance Hospital (IRB approval number: 3-2011-0191).

Plasmids. Each of the two shRNA-encoding oligonucleotides against human TrkC and c-Src were designed and verified to be specific to TrkC and c-Src by BLAST searches against the mouse and human genomes, respectively. The primers corresponding to shRNA against TrkC and c-Src were cloned into the pLKO lentiviral vector to generate the TrkC-shRNA expression plasmid (Table S3). A control shRNA that did not match any known mouse- or human-coding cDNA was used as a control.

Antibodies, western blotting, immunoprecipitation, and immunofluorescence. We performed western blotting, immunoprecipitation, and immunofluorescence analysis as previously described[33]. Anti-IL-6 neutralizing antibody (mabg-hil6-3) was from InvivoGen; Anti-HA (SC-805), anti-TrkC (SC-117), and anti-Myc (SC-40) were from Santa Cruz Biotechnology; anti-V5 (R960-CUS) was from Invitrogen; anti-SOCS3 (ab16030), anti-JAK2 (ab108596), anti-Twist-1 (ab50887), and anti-phosphotyrosine (ab10321) were from Abcam; anti-STAT3 (9139), anti-phospho-STAT3 (4113), and anti-phospho-JAK2 (3771) were from Cell Signaling Technology; and anti-E-cadherin (610405), anti-fibronectin (610078), anti-N-cadherin (610920), anti-alpha-catenin (610194), and anti-beta-catenin (610154) were from BD Transduction.

Soft agar assays, wound healing assays, anchorage-independent cell growth, viral production, reverse transcription PCR, and matrigel invasion assays. All of the assays were performed as previously described[33,54]. The primer sequences used to amplify the genes are listed in the supplemental experimental procedures (Table S4).

Quantitative RT-PCR. The primer sequences are listed in the supplemental experimental procedures (Table S4). Total RNA was isolated using RNeasy Mini Kits (Qiagen) according to the manufacturer's instructions and reverse transcribed with Hexa-nucleotide Mix (Roche). The resulting cDNA was subjected to PCR using the SYBR-Green Master PCR mix and the Taqman master PCR mix (Applied Biosystems) in triplicate. PCR and data collection were performed using the 7900HT Fast Real-Time PCR System (Applied Biosystems). All quantitations were normalized to the endogenous control 18S RNA. Specific TrkC (Hs00176797_m1) and 18S (Hs99999901_s1) quantitative probes for Taqman RT-PCR were obtained from Applied Biosystems.

Luciferase reporter assay. Cells that were 50% confluent in 12-well dishes were transfected using Lipofectamine 2000 (Invitrogen). A total of 0.5 μg E-cadherin, Twist-1, Twist-2, or STAT3 reporter gene constructs and 0.5 μg of pCMV-β-gal were cotransfected per well. The cell extracts were prepared 48 hrs after transfection, and luciferase activity was quantified using the Enhanced Luciferase Assay Kit (BD Biosciences). All of the experiments were performed in triplicate.

ELISA assay. Equal numbers of Hs578T control-shRNA or Hs578T TrkC-shRNA cells were plated and cultured for 3 days. Subsequently, conditioned media from these cell cultures were collected and analyzed by the Human IL-6 Quantikine ELIZA kit (R&D systems) according to the manufacturer's instructions.

Microarray data analysis. TrkC and Twist-1 levels in 2,136 breast cancer patients of the Curtis database[34] and 158 breast cancer patients of the Gluck database[60] were extracted and averaged. ANOVA was performed and boxplot graphs were plotted with gene expression using GraphPad Prism v 5.0 (GraphPad Software, Inc.). A $P < 0.0001$ was considered to indicate significance.

Animal studies. Animal studies were performed as previously described[33]. Female BALB/c Nu/Nu mice (7 weeks old) were purchased from the Korea Research Institute of Bioscience and Biotechnology (KRIBB, South Korea) and handled in compliance with protocols approved by the Institutional Animal Care and Use Committee (IACUC) of Gachon University (Approval No. LCDI-2012-0016). For tumorigenicity studies, Hs578T (1×10^5), MCF10A-Ras (1×10^6), or MCF10A-Ras-TrkC (1×10^6) cells suspended in 50μl PBS/Matrigel (BD Biosciences) were injected subcutaneously into the left and right hind flank regions under anesthesia. Mice were euthanized at indicated days, and primary tumors were excised for analysis. For tail-vein injection, 1×10^5 cells suspended in 50μl PBS were injected into the tail vein of 7-week-old female BALB/c Nu/Nu mice. For tumor inhibition by LOXO-101 (Active Biochem), Hs578T cells (1×10^6) were injected subcutaneously into the dorsal flank area of the mice. Once tumors were established and reached a size of $200 \pm 20\,mm^3$, LOXO-101 (60 mg/kg/dose) was administrated by oral gavage twice daily for 14 days.

Statistical analysis. Data are expressed as the mean ± SEM. Statistical analyses of data were conducted via Student's t test (two-tailed) and ANOVA. Differences were considered statistically significant at $P < 0.05$ or $P < 0.0001$.

References

1. Hennessy, B. T. *et al.* Characterization of a naturally occurring breast cancer subset enriched in epithelial-to-mesenchymal transition and stem cell characteristics. *Cancer research* **69,** 4116–4124 (2009).
2. Hanahan, D. & Weinberg, R. A. Hallmarks of cancer: the next generation. *Cell* **144,** 646–674 (2011).
3. Kalluri, R. & Weinberg, R. A. The basics of epithelial-mesenchymal transition. *The Journal of clinical investigation* **119,** 1420–1428 (2009).
4. Batlle, E. *et al.* The transcription factor snail is a repressor of E-cadherin gene expression in epithelial tumour cells. *Nat Cell Biol* **2,** 84–89 (2000).
5. Cano, A. *et al.* The transcription factor snail controls epithelial-mesenchymal transitions by repressing E-cadherin expression. *Nat Cell Biol* **2,** 76–83 (2000).
6. Carver, E. A., Jiang, R., Lan, Y., Oram, K. F. & Gridley, T. The mouse snail gene encodes a key regulator of the epithelial-mesenchymal transition. *Mol Cell Biol* **21,** 8184–8188 (2001).
7. Nieto, M. A., Sargent, M. G., Wilkinson, D. G. & Cooke, J. Control of cell behavior during vertebrate development by Slug, a zinc finger gene. *Science* **264,** 835–839 (1994).
8. Savagner, P., Yamada, K. M. & Thiery, J. P. The zinc-finger protein slug causes desmosome dissociation, an initial and necessary step for growth factor-induced epithelial-mesenchymal transition. *J Cell Biol* **137,** 1403–1419 (1997).
9. Comijn, J. *et al.* The two-handed E box binding zinc finger protein SIP1 downregulates E-cadherin and induces invasion. *Mol Cell* **7,** 1267–1278 (2001).
10. Vandewalle, C. *et al.* SIP1/ZEB2 induces EMT by repressing genes of different epithelial cell-cell junctions. *Nucleic Acids Res* **33,** 6566–6578 (2005).
11. Perez-Moreno, M. A. *et al.* A new role for E12/E47 in the repression of E-cadherin expression and epithelial-mesenchymal transitions. *J Biol Chem* **276,** 27424–27431 (2001).
12. Hartwell, K. A. *et al.* The Spemann organizer gene, Goosecoid, promotes tumor metastasis. *Proc Natl Acad Sci USA* **103,** 18969–18974 (2006).
13. Mani, S. A. *et al.* Mesenchyme Forkhead 1 (FOXC2) plays a key role in metastasis and is associated with aggressive basal-like breast cancers. *Proceedings of the National Academy of Sciences of the United States of America* **104,** 10069–10074 (2007).
14. Yang, J. *et al.* Twist, a master regulator of morphogenesis, plays an essential role in tumor metastasis. *Cell* **117,** 927–939 (2004).
15. Ansieau, S. *et al.* Induction of EMT by twist proteins as a collateral effect of tumor-promoting inactivation of premature senescence. *Cancer cell* **14,** 79–89 (2008).
16. Ailles, L. E. & Weissman, I. L. Cancer stem cells in solid tumors. *Current opinion in biotechnology* **18,** 460–466 (2007).
17. Chaffer, C. L. *et al.* Normal and neoplastic nonstem cells can spontaneously convert to a stem-like state. *Proceedings of the National Academy of Sciences of the United States of America* **108,** 7950–7955 (2011).
18. Marotta, L. L. *et al.* The JAK2/STAT3 signaling pathway is required for growth of CD44(+)CD24(−) stem cell-like breast cancer cells in human tumors. *The Journal of clinical investigation* **121,** 2723–2735 (2011).
19. Chao, M. V. & Bothwell, M. Neurotrophins: to cleave or not to cleave. *Neuron* **33,** 9–12 (2002).
20. Grotzer, M. A. *et al.* TrkC expression predicts good clinical outcome in primitive neuroectodermal brain tumors. *Journal of clinical oncology: official journal of the American Society of Clinical Oncology* **18,** 1027–1035 (2000).
21. Hisaoka, M., Sheng, W. Q., Tanaka, A. & Hashimoto, H. Gene expression of TrkC (NTRK3) in human soft tissue tumours. *J Pathol* **197,** 661–667 (2002).
22. Ricci, A. *et al.* Neurotrophins and neurotrophin receptors in human lung cancer. *Am J Respir Cell Mol Biol* **25,** 439–446 (2001).
23. Yamashiro, D. J. *et al.* Expression and function of Trk-C in favourable human neuroblastomas. *Eur J Cancer* **33,** 2054–2057 (1997).
24. Stephens, P. *et al.* A screen of the complete protein kinase gene family identifies diverse patterns of somatic mutations in human breast cancer. *Nature genetics* **37,** 590–592 (2005).

25. Greenman, C. *et al.* Patterns of somatic mutation in human cancer genomes. *Nature* **446,** 153–158 (2007).
26. Davies, H. *et al.* Somatic mutations of the protein kinase gene family in human lung cancer. *Cancer research* **65,** 7591–7595 (2005).
27. Bardelli, A. *et al.* Mutational analysis of the tyrosine kinome in colorectal cancers. *Science* **300,** 949 (2003).
28. Kubo, T. *et al.* Resequencing analysis of the human tyrosine kinase gene family in pancreatic cancer. *Pancreas* **38,** e200–206 (2009).
29. Jones, S. *et al.* Core signaling pathways in human pancreatic cancers revealed by global genomic analyses. *Science* **321,** 1801–1806 (2008).
30. Wood, L. D. *et al.* Somatic mutations of GUCY2F, EPHA3, and NTRK3 in human cancers. *Hum Mutat* **27,** 1060–1061 (2006).
31. Jin, W., Yun, C., Kwak, M. K., Kim, T. A. & Kim, S. J. TrkC binds to the type II TGF-beta receptor to suppress TGF-beta signaling. *Oncogene* **26,** 7684–7691 (2007).
32. Jin, W. *et al.* c-Src is required for tropomyosin receptor kinase C (TrkC)-induced activation of the phosphatidylinositol 3-kinase (PI3K)-AKT pathway. *J Biol Chem* **283,** 1391–1400 (2008).
33. Jin, W. *et al.* TrkC plays an essential role in breast tumor growth and metastasis. *Carcinogenesis* **31,** 1939–1947 (2010).
34. Curtis, C. *et al.* The genomic and transcriptomic architecture of 2,000 breast tumours reveals novel subgroups. *Nature* **486,** 346–352 (2012).
35. Croker, B. A., Kiu, H. & Nicholson, S. E. SOCS regulation of the JAK/STAT signalling pathway. *Seminars in cell & developmental biology* **19,** 414–422 (2008).
36. Sansone, P. *et al.* IL-6 triggers malignant features in mammospheres from human ductal breast carcinoma and normal mammary gland. *The Journal of clinical investigation* **117,** 3988–4002 (2007).
37. Bromberg, J. & Wang, T. C. Inflammation and cancer: IL-6 and STAT3 complete the link. *Cancer cell* **15,** 79–80 (2009).
38. Matsuda, T. *et al.* STAT3 activation is sufficient to maintain an undifferentiated state of mouse embryonic stem cells. *The EMBO journal* **18,** 4261–4269 (1999).
39. Iliopoulos, D., Hirsch, H. A., Wang, G. & Struhl, K. Inducible formation of breast cancer stem cells and their dynamic equilibrium with non-stem cancer cells via IL6 secretion. *Proceedings of the National Academy of Sciences of the United States of America* **108,** 1397–1402 (2011).
40. Korkaya, H. *et al.* Activation of an IL6 inflammatory loop mediates trastuzumab resistance in HER2+breast cancer by expanding the cancer stem cell population. *Mol Cell* **47,** 570–584 (2012).
41. Cheng, G. Z. *et al.* Twist is transcriptionally induced by activation of STAT3 and mediates STAT3 oncogenic function. *J Biol Chem* **283,** 14665–14673 (2008).
42. Polyak, K. & Weinberg, R. A. Transitions between epithelial and mesenchymal states: acquisition of malignant and stem cell traits. *Nature reviews. Cancer* **9,** 265–273 (2009).
43. Thiery, J. P. Epithelial-mesenchymal transitions in tumour progression. *Nature reviews. Cancer* **2,** 442–454 (2002).
44. Thuault, S. *et al.* HMGA2 and Smads co-regulate SNAIL1 expression during induction of epithelial-to-mesenchymal transition. *J Biol Chem* **283,** 33437–33446 (2008).
45. Mani, S. A. *et al.* The epithelial-mesenchymal transition generates cells with properties of stem cells. *Cell* **133,** 704–715 (2008).
46. Raval, A. *et al.* TWIST2 demonstrates differential methylation in immunoglobulin variable heavy chain mutated and unmutated chronic lymphocytic leukemia. *Journal of clinical oncology: official journal of the American Society of Clinical Oncology* **23,** 3877–3885 (2005).
47. Doebele, R. C. *et al.* An Oncogenic NTRK Fusion in a Patient with Soft-Tissue Sarcoma with Response to the Tropomyosin-Related Kinase Inhibitor LOXO-101. *Cancer discovery* **5,** 1049–1057 (2015).
48. Croker, B. A. *et al.* SOCS3 negatively regulates IL-6 signaling *in vivo*. *Nature immunology* **4,** 540–545 (2003).
49. Lang, R. *et al.* SOCS3 regulates the plasticity of gp130 signaling. *Nature immunology* **4,** 546–550 (2003).
50. Jones, S. A., White, C. A., Robb, L., Alexander, W. S. & Tarlinton, D. M. SOCS3 deletion in B cells alters cytokine responses and germinal center output. *J Immunol* **187,** 6318–6326 (2011).
51. Sutherland, K. D., Lindeman, G. J. & Visvader, J. E. Knocking off SOCS genes in the mammary gland. *Cell Cycle* **6,** 799–803 (2007).
52. Scheel, C. *et al.* Paracrine and autocrine signals induce and maintain mesenchymal and stem cell states in the breast. *Cell* **145,** 926–940 (2011).
53. Nagata, Y. *et al.* PTEN activation contributes to tumor inhibition by trastuzumab, and loss of PTEN predicts trastuzumab resistance in patients. *Cancer cell* **6,** 117–127 (2004).
54. Lu, J. *et al.* 14-3-3zeta Cooperates with ErbB2 to promote ductal carcinoma in situ progression to invasive breast cancer by inducing epithelial-mesenchymal transition. *Cancer cell* **16,** 195–207 (2009).
55. Fidler, I. J. The pathogenesis of cancer metastasis: the 'seed and soil' hypothesis revisited. *Nature reviews. Cancer* **3,** 453–458 (2003).
56. Hoek, K. *et al.* Expression profiling reveals novel pathways in the transformation of melanocytes to melanomas. *Cancer research* **64,** 5270–5282 (2004).
57. Maestro, R. *et al.* Twist is a potential oncogene that inhibits apoptosis. *Genes Dev* **13,** 2207–2217 (1999).
58. Rosivatz, E. *et al.* Differential expression of the epithelial-mesenchymal transition regulators snail, SIP1, and twist in gastric cancer. *Am J Pathol* **161,** 1881–1891 (2002).
59. Fillmore, C. M. & Kuperwasser, C. Human breast cancer cell lines contain stem-like cells that self-renew, give rise to phenotypically diverse progeny and survive chemotherapy. *Breast cancer research: BCR* **10,** R25 (2008).
60. Gluck, S. *et al.* TP53 genomics predict higher clinical and pathologic tumor response in operable early-stage breast cancer treated with docetaxel-capecitabine+/− trastuzumab. *Breast cancer research and treatment* **132,** 781–791 (2012).

Acknowledgements

We thank R. Park for the critical reading of the manuscript. This work was supported by a National Research Foundation of Korea grant (NRF-2010-0002525, NRF-2012R1A2A2A01002728 to W.J. and 2015R1D1A1A01059406 to M.S.K.), the Gachon University Gil Medical Center (2014-14 to W. J.), and by grant Bio & Medical Technology Development Program (NRF-2014M3A9B5073918 to S.-J.K) of the Ministry of Science, ICT and Future Planning through the National Research Foundation, Korea.

Author Contributions

M.S.K., S.-J.K. and W.J. designed research; M.S.K., J.S., J.J. and H.-S.K. performed research; M.S.K., H.-S.K., S.-J.K. and W.J. analyzed data; and S.-J.K. and W.J. wrote the main manuscript text.

Additional Information

Supplementary information accompanies this paper at http://www.nature.com/srep

Competing financial interests: The authors declare no competing financial interests.

How to cite this article: Kim, M. S. *et al.* Dysregulated JAK2 expression by TrkC promotes metastasis potential, and EMT program of metastatic breast cancer. *Sci. Rep.* **6**, 33899; doi: 10.1038/srep33899 (2016).